JACS
JOURNAL OF THE AMERICAN CHEMICAL SOCIETY
pubs.acs.org/JACS
Article

Constitutional Dynamic Selection at Low Reynolds Number in a Triple Dynamic System: Covalent Dynamic Adaptation Driven by Double Supramolecular Self-Assembly

Ruirui Gu and Jean-Marie Lehn*

Cite This: https://doi.org/10.1021/jacs.1c04446
Read Online

ABSTRACT: A triple dynamic complex system has been designed, implementing a dynamic covalent process coupled to two supramolecular self-assembly steps. To this end, two dynamic covalent libraries (DCLs), **DCL-1** and **DCL-2**, have been established on the basis of dynamic covalent C═C/C═N organo-metathesis between two Knoevenagel derivatives and two imines. Each DCL contains a barbituric acid-based Knoevenagel constituent that may undergo a sequential double self-organization process involving first the formation of hydrogen-bonded hexameric supramolecular macrocycles that subsequently undergo stacking to generate a supramolecular polymer SP yielding a viscous gel state. Both DCLs display selective self-organization-driven amplification of the constituent that leads to the SP. Dissociation of the SP on heating causes reversible randomization of the constituent distributions of the DCLs as a function of temperature. Furthermore, diverse distribution patterns of **DCL-2** were induced by modulation of temperature and solvent composition. The present dynamic systems display remarkable self-organization-driven constitutional adaption and tunable composition by coupling between dynamic covalent component selection and two-stage supramolecular organization. In more general terms, they reveal dynamic adaptation by component selection in low Reynolds number conditions of living systems where frictional effects dominate inertial behavior.

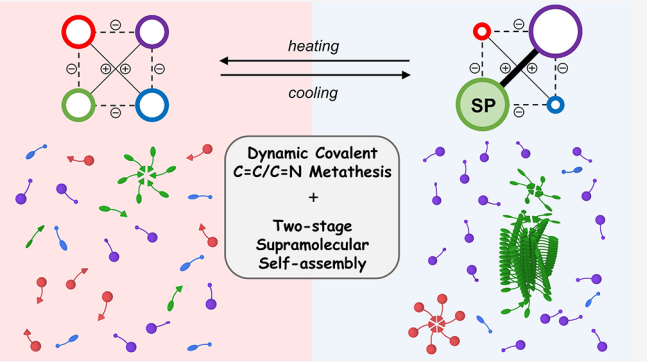

INTRODUCTION

In the famous paper "Life at Low Reynolds Number", Edward Purcell pointed out that living systems operate in conditions where frictional effects strongly dominate inertial features.[1] Purcell had a major role in the development of NMR, particularly in its nuclear relaxation aspect,[2] which bears direct dependence on molecular motions and thus on frictional effects. These relationships establish a connection between nuclear relaxation and supramolecular organization as embodied in medium viscosity. As a consequence, chemical systems might be able to change/adapt their constitution under the driving force of an increase in organization.

Considering that frictional effects result from intermolecular interactions and determine bulk properties such as viscosity, an increase in viscosity corresponds to higher supramolecular (passive) self-organization.[3] It would thus be of great interest to devise chemical systems whose behavior would reveal the driving force of self-organization[4] by inducing the generation of just the very chemical entity that leads to higher organization in a sort of organizational autocatalytic process. Such would be the case if the increase in organization occurring on transition from a solution to a gel state were to enforce the amplification of the gel forming entity, thus revealing the organizational power of a soft matter, complex fluid medium[5] as characterized by bulk properties, viscosity and therefore low Reynolds number conditions. Constitutional dynamic chemistry (CDC)[6] offers such perspectives. It is for these relationships that we wish to dedicate the present study to the memory of Edward Purcell.[1]

RATIONALE

CDC rests on the generation of dynamic libraries of molecular (covalent) or supramolecular (noncovalent) constituents by recombination of their components linked, respectively, by reversible chemical bonds or intermolecular interactions or by both simultaneously. In response to the application of physical stimuli or chemical effectors, such complex dynamic systems may undergo constitutional changes through selection of the

Received: May 4, 2021

appropriate components and display adaptation to the acting agent.

The implementation of CDC at the molecular level, that is, dynamic covalent chemistry (DCC), involves reversible reactions and generates dynamic covalent libraries (DCLs) in which the relationships between constituents are described by an underlying constitutional dynamic network (CDN). Such reactions include amine/carbonyl condensations,[6] disulfide exchange,[6b,c,7] peptide exchange,[8] olefin metathesis,[9] and Diels–Alder condensation.[10] Furthermore, the C=C/C=N organo-metathesis taking place between Knoevenagel (Kn) compounds derived from 1,3-dimethylbarbituric acid and imines (aldimines or Schiff bases) in low polar organic solvents was found to be an efficient way to establish DCLs (Scheme 1a).[11] One may note that the well-balanced

Scheme 1. (a) Component Exchange between Knoevenagel Barbituric Derivatives to Undergo Component Exchange with Imines (or Schiff Bases) by C=C/C=N Organo-metathesis; (b) Hexameric Hydrogen-Bonded Supramolecular Macrocycle ("Rosette") Formation (Left to Center) Followed by a Second Self-Assembly to Generate a Supramolecular Polymer SP by Stacking of the Rosettes (Center to Right) in a Double Supramolecular Process; (Right) Simplified "Artist" Representation of SP; and (c) Steric Hindrance to Stacking Polymerization of the "Rosette" Assembly[a]

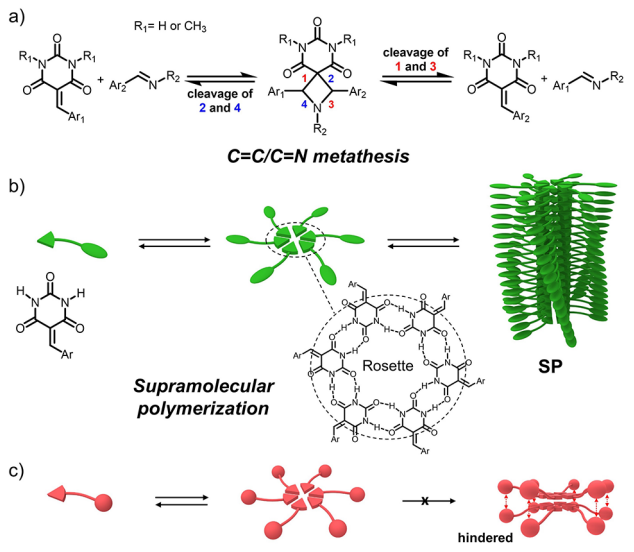

[a]**Kn1**, **Kn2**, and **Kn3** form all three of the "rosettes", but subsequent polymerization to SP is hindered for **Kn1** by the bulky adamantane groups in the R1 side chains (see Scheme 2a).

Knoevenagel/imine reversible exchange also represents a very sensitive touchstone for the quantitative evaluation of the forces acting on the equilibrating system and shifting the equilibrium position.

The lability of noncovalent interactions allows for the establishment of constitutional dynamic systems at the supramolecular level. Such interactions may drive the formation of more or less highly organized supramolecular entities by recognition between their complementary molecular components.[12−15] The resulting self-organization ability (passive, equilibrium) leads to the generation of complex architectures with component selection and adaptation in response to the application of diverse external (environmental) agents. Hydrogen bonding, electrostatic, and van der Waals interactions play a major role in the buildup of biological architectures, for instance, of the double helix structure of nucleic acids or the assembling of polypeptide chains in proteins. To implement such elaborate processes, to expand on them, and to create functional materials with diverse chemical or physical properties, numerous chemical structures of various types have been designed and synthesized, involving in particular multiple hydrogen-bonding motifs.[13−15] Among the latter, derivatives of barbituric acid or analogues have been demonstrated to be able to form sextuple hydrogen-bonding patterns with a complementary receptor moiety and undergo supramolecular polymerization,[13h−j] as well as form hydrogen-bonded macrocyclic hexamers (rosettes) that may assemble into supramolecular polymeric stacks.[13d−g,15]

In this Article, we describe constitutional dynamic systems that involve a triple dynamic process, a dynamic covalent component exchange based on C=C/C=N organo-metathesis followed by two sequential supramolecular assembly steps (formation of rosettes and their self-assembly into polymeric stacks). We demonstrate the direct correlation between the degree of molecular organization (as displayed by viscosity and measured by corresponding ^{1}H NMR signal line width) and amplification by component selection of the constituent that yields higher order in a self-organization driven mode.[16] It represents a direct demonstration of the spontaneous trend of "passive" self-organization to drive selection and thus, in Purcell's terms, low Reynolds number driving chemical selection, both being characteristic features of living systems.

We have shown earlier in systems involving supramolecular organization linked to a dynamic covalent process that indeed the possibility of the formation of a gel causes the selection of just those components that generate the very constitution that yields the gel.[6a,16a,d] Thus, a high friction/low Reynolds number marks an increase in medium organization, which drives component selection and constituent adaptation.

Here, we implement two four-membered DCLs that take advantage of the dynamic covalent organo-metathesis reactivity of Kn compounds with imines to generate library constituents capable of undergoing hierarchical two-level supramolecular self-assembly, the initial formation of discrete hydrogen-bonded hexameric rosettes and their subsequent stacking to give a cylindrical supramolecular polymer (Scheme 1b). Driven by supramolecular self-organization under temperature modulation, the distributions of the DCLs form a constitutional dynamic network that displays variation from a four-member-statistically averaged state to constitutionally selected states (Scheme 2b). Such selection could be reversibly switched by heating/cooling of the reaction mixture. The distributions of the libraries were investigated by ^{1}H NMR and UV–vis spectroscopy, while the supramolecular polymeric entities were characterized by DLS, AFM, and cryo-TEM.

RESULTS AND DISCUSSION

Two DCLs were investigated: **DCL-1** consisting of **Kn1**, **A1**, **Kn2**, and **A2**, and **DCL-2** consisting of **Kn1**, **A1**, **Kn3**, and **A3** (Scheme 2a). **DCL-1′** and **DCL-2′**, involving *N*-methylated barbituric groups, which cannot undergo association by H-bonding, were studied for comparison with the libraries **DCL-1** and **DCL-2**, respectively. Detailed synthetic procedures and

https://doi.org/10.1021/jacs.1c04446
J. Am. Chem. Soc. XXXX, XXX, XXX−XXX

Scheme 2. (a) The Two Dynamic Combinatorial Libraries DCL-1 and DCL-2 Composed Each of Four Constituents; and (b) (Left) Component Exchange between the Agonistic Constituents Kn1/A*x* or Kn*x*/A1 by Organo-metathesis (Scheme 1a), Generating the Same Equilibrated [2 × 2] Square Constitutional Dynamic Network (CDN) with (Center) No Constitutional Selection; (Right) The CDN Undergoes Reversible Amplification of Kn*x* and of Its Agonist A1 as a Function of Temperature, Driven by Self-Organization-Induced Constitutional Selection on Formation of SP[a]

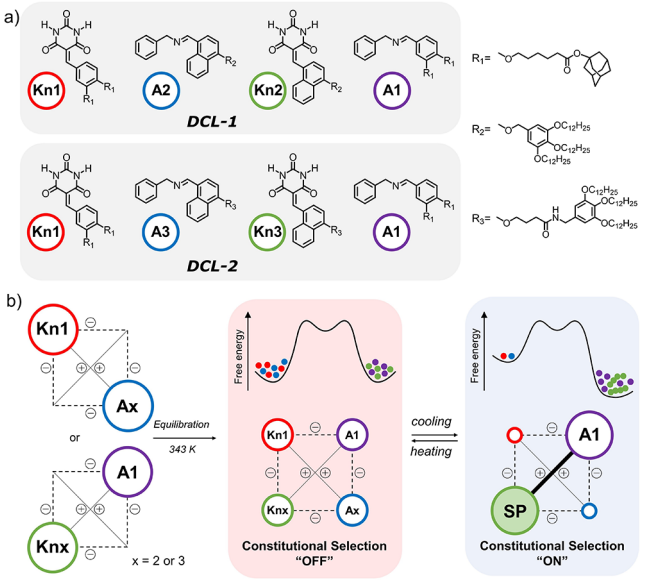

[a]For **A*x*** and **Kn*x***, *x* = 2 or 3.

characterization data of all of the compounds are presented in the Supporting Information.

Design of the Constituents and Generation of the DCLs. It has been reported that Knoevenagel condensation products of barbituric acid and aromatic aldehyde components form six-member rosettes connected by double hydrogen bonding and then undergo polymerization via stacking of the rosette layers in low-polarity solvents (for example, hexane and methylcyclohexane).[15] It has also been shown that Knoevenagel derivatives perform dynamic covalent component exchange with imines catalyzed by L-proline.[11a] However, due to their low solubility, these exchange processes had to be run in dimethyl sulfoxide. For the present purposes, the Knoevenagel compounds were thus equipped with aliphatic chains to reach sufficient solubility in solvents of low polarity. Indeed, it has been confirmed in this work that they do undergo the C═C/C═N exchange in chloroform without a catalyst (Scheme 1a).

On the basis of these studies, compounds **Kn1** and **Kn2** were used to generate the four constituents of **DCL-1** by reaction with their imine agonists **A2** and **A1**, respectively (Scheme 2b, left). Another library **DCL-2** was designed to induce better constitutional selectivity. It was envisaged that the extra $-C_3H_6CONH-$ fragment present in the side chains of compound **Kn3** would lead to the formation of intermolecular hydrogen bonds between the amide units and thus generate supramolecular architectures of higher thermodynamic stability, as has been reported.[14d,e] Both **DCL-1** and **DCL-2** form a square CDN linking their four constituents.

Compound **Kn1**, present in both DCLs, was chosen as a 3,4-disubstituted structure to ensure better solubility in nonpolar solvents. It was also equipped with two adamantane groups expecting that their steric bulk would hinder the formation of supramolecular polymeric assemblies by stacking of **Kn1**-based hexameric rosettes (Scheme 1c) and thus reduce their thermodynamic stability, so as to create a difference in free energy between reactants and exchange products. The four-member DCLs were obtained by mixing two diagonally related agonistic constituents or the orthogonal ones in the chosen solvent. Thus, for **DCL-1**, an equimolar mixture of **Kn1**+**A2** gave the same distribution of constituents as **Kn2**+**A1** after equilibration. One may expect that at a temperature high enough to dissociate the hydrogen-bonded aggregates, the four constituents would be present as monomers with a statistical distribution of about 25% each. Upon cooling of the reaction mixture, the monomeric Knoevenagel derivatives **Kn1** and **Kn2** (or **Kn3**) would start to assemble and coassemble into hexameric rosette supramolecular macrocycles, followed by self-organization and self-sorting of the coaggregated rosettes into **Kn2** (or **Kn3**)-dominated supramolecular polymers as a consequence of the lower thermodynamic stability of **Kn1** assemblies. Meanwhile, the difference in free energy would be expected to drive the C═C/C═N metathesis reaction to favor the formation of **Kn2** (or **Kn3**) and its agonist **A1**, resulting in a constitutionally selected mixture. The process is expected to be reversible with randomization on temperature increase.

Medium. Chloroform/cyclohexane ($CHCl_3$/CH) or 1,1,2,2-tetrachloroethane/methylcyclohexane ($C_2H_2Cl_4$/MCH; for studies at higher temperatures) mixtures were chosen as the reaction medium for the present DCLs. The Knoevenagel/imine C═C/C═N exchange reaction is known to be fast in chloroform.[11b] Regarding the effect of solvent on H-bonding-based self-assembly, one expects that the addition of a low polarity solvent increases the degree of aggregation and strengthens the thermodynamic stability of the supramolecular polymers.[14f] The ratio of the two solvents was tuned according to the specific situation as it is an important parameter of the DCLs affecting not only the equilibration rate but also the constitutional selectivity.

Dynamic Covalent Library-1 (DCL-1). A solution of 2 mM **Kn1** + **A2** in 20% $CDCl_3$ + 80% CH-d_{12} was allowed to equilibrate at 343 K and monitored by ^{1}H NMR. After the equilibrium was reached, all four constituents could be observed in the spectrum, the distribution being essentially statistical with about 25% of each constituent **Kn1**, **A2**, **Kn2**, and **A1** (**A1**:**A2** = 1:1.04; see Figure S1a for the ^{1}H NMR spectrum). As the mixture was gradually cooled to 293 K at a rate 0.5 K/min, the ^{1}H NMR peaks of the two **Kn** compounds became broad and unobservable, which indicated the formation of supramolecular self-assemblies. The equilibrium state at 293 K was reached in about 33 h. The ratio of **A1**:**A2** became 1:0.91 (Figure S1b). As compared to the distribution at 343 K, the equilibrium of the reaction had undergone a small shift. It should be noted that, in this case and most of the other cases presented below, the NMR signals of the Kn compounds (**Kn1**, **Kn2**, and **Kn3**) were rarely observable because of the supramolecular assembly and coassembly. Under these circumstances, the distributions of the constituents of the libraries can be inferred from the ratio of the two imines **A1** and **A2**, which do not participate in the supramolecular aggregates.

https://doi.org/10.1021/jacs.1c04446
J. Am. Chem. Soc. XXXX, XXX, XXX−XXX

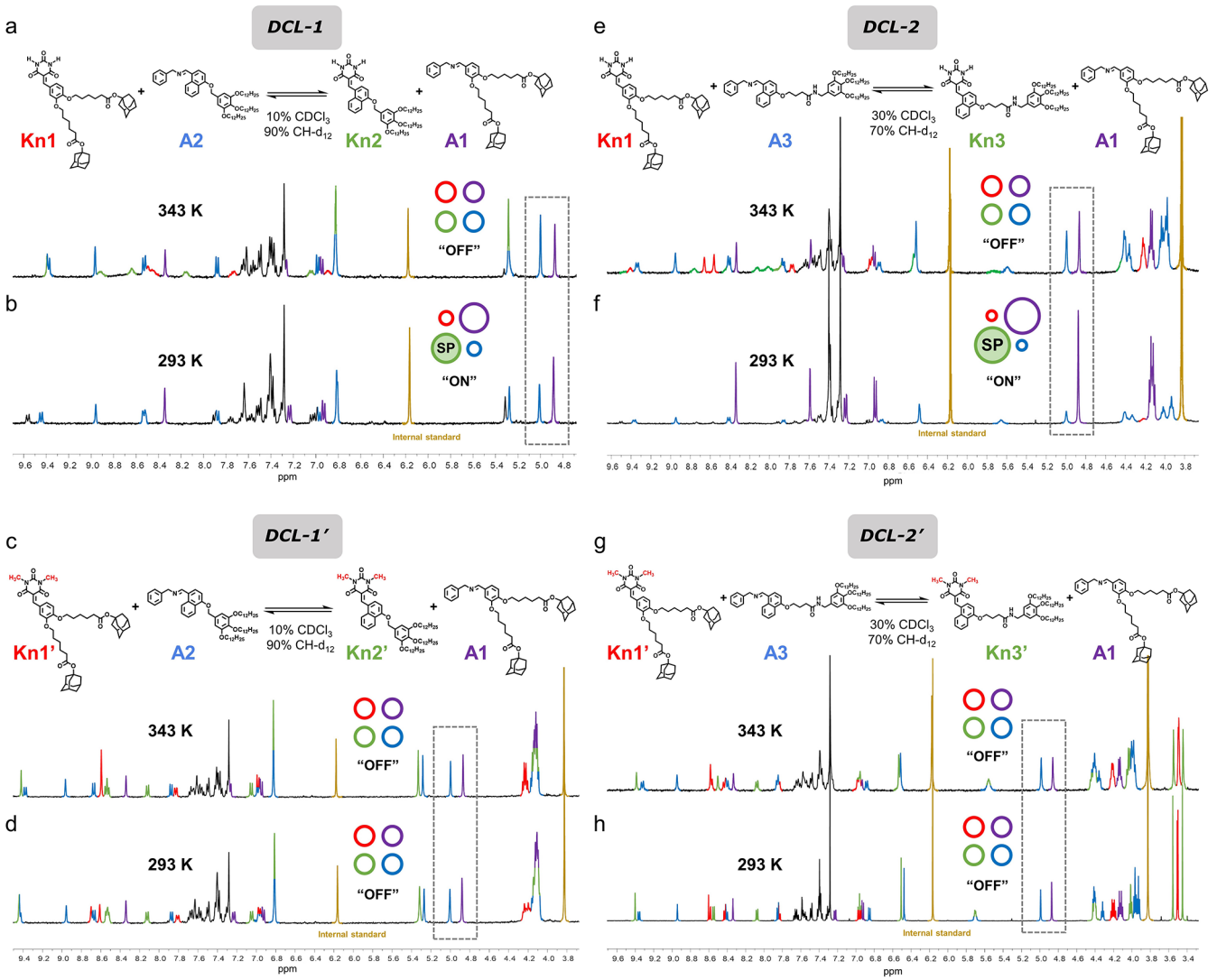

Figure 1. 400 MHz ^{1}H NMR spectra of the equilibrated solutions of 2 mM **DCL-1** in 10% $CDCl_3$ + 90% CH-d_{12} (a) at 343 K and (b) at 293 K; 2 mM **DCL-1′** in 10% $CDCl_3$ + 90% CH-d_{12} (c) at 343 K and (d) at 293 K; 2 mM **DCL-2** in 30% $CDCl_3$ + 70% CH-d_{12} (e) at 343 K and (f) at 293 K; and 2 mM **DCL-2′** in 10% $CDCl_3$ + 90% CH-d_{12} (g) at 343 K and (h) at 293 K. SP: supramolecular polymer. Benzyl $-CH_2-$ signals of the two imines in each DCL are highlighted in the dashed gray boxes, and their ratio indicates the "ON" or "OFF" state of the DCLs. The error in signal integration amounts to about 5%.

DCL-1 in 10% $CDCl_3$ + 90% CH-d_{12} was submitted to the same procedure, the less polar solvent being expected to strengthen the driving force of self-assembly. At 343 K, the ^{1}H NMR peaks of both **Kn1** and **Kn2** were broad and difficult to integrate. In the equilibrated solution, the **A1**:**A2** ratio was 1:1.03 (Figure 1a). Cooling to 293 K caused a progressive amplification of **A1** and a reduction of **A2**. After 106 h (indicating a much slower rate due to the lower solvent polarity), the equilibrium was reached, and the ratio of **A1**:**A2** became 1:0.6 (Figure 1b). Meanwhile, 22% of aldehyde hydrolysis products were detected as indicated by the CHO ^{1}H NMR proton signal. Comparing these two cases, the change in reaction medium from 20% $CDCl_3$ to 10% affected the DCL by slowing the reaction rate and inducing a larger shift in the equilibrium toward the formation of **Kn2** and **A1**.

DCL-1′, containing the bis-*N*-methylated Knoevenagel compounds **Kn1′** and **Kn2′** in place of **Kn1** and **Kn2** (see Figure 1c), was investigated in 10% $CDCl_3$ + 90% CH-d_{12} as a case comparative to **DCL-1**. The structures of the four constituents **Kn1′**, **A2**, **Kn2′**, and **A1** are shown in Figure 1c. After the equilibration of a 2 mM **Kn1′** + **A2** solution at 343 K, a mixture of 24% **Kn1′**, 23% **A2**, 27% **Kn2′**, and 26% **A1** was obtained (Figure 1c). On cooling to 293 K, all four constituents remained clearly observable, while the thermodynamic equilibrium reached 12 h later indicated only a slight variation in distribution (23% **Kn1′**, 22% **A2**, 28% **Kn2′**, and 27% **A1**, with less than 5% hydrolysis; see the spectrum in Figure 1d). In this DCL, the introduction of two methyl groups on the barbituric rings of the **Kn** compounds prevented them from self-assembling, resulting in the disruption of the constitutional selectivity in this library.

Dynamic Covalent Library-2 (DCL-2). The two reactants **Kn1** and **A3** (2 mM each) were mixed in 10% $CDCl_3$ + 90% CH-d_{12} and allowed to equilibrate at 343 K to give the four-member mixture, **DCL-2**. The ^{1}H NMR spectrum at equilibrium gave **A1**:**A3** as 1:0.15, while **Kn1** and **Kn3** peaks were not observable (Figure S2a). In contrast to **DCL-1**, the exchange products **Kn3** and **A1** were already selected as the main species. The equilibrium mixture obtained 20 h after mixing was cooled to 293 K to give **A1**:**A3** as 1:0.13 (Figure

https://doi.org/10.1021/jacs.1c04446
J. Am. Chem. Soc. XXXX, XXX, XXX−XXX

S2b). The considerable thermodynamic stability of **Kn3** indicated by these distributions at the two equilibrium states is much stronger than that of **Kn2** and may be attributed to the extra intermolecular hydrogen bonding between the amide units.

However, to optimize the aggregation-induced variation of distribution, the effect of the composition of the reaction medium (the ratio of $CDCl_3$ and CH-d_{12}) on the behavior of **Kn3** was explored by titration of $CDCl_3$ into a CH-d_{12} solution of **Kn3** at 293 K (see Figure S3 for the ^{1}H NMR spectra). At the beginning (15% $CDCl_3$ + 85% CH-d_{12}), only aliphatic chains in the low ppm region of the ^{1}H NMR spectrum could be detected. On increasing the fraction of $CDCl_3$, the signals at high ppm values started to show up (30% $CDCl_3$ + 70% CH-d_{12}). After the $CDCl_3$ proportion reached 50%, all of the peaks became narrow and clear. During the titration process, the **Kn3** solution always remained transparent. This titration experiment indicated, as expected, the negative influence of $CDCl_3$ on the self-assembly of compound **Kn3** and suggested that a composition of 30% $CDCl_3$ + 70% CH-d_{12} could be a suitable medium for **DCL-2**.

To confirm the effect of solvent polarity on the dynamic library, a series of **DCL-2** reactions were conducted in media of five different $CDCl_3$:CH-d_{12} compositions. The corresponding distributions obtained at 343 and 293 K are illustrated in Figure 2. The equilibration was slowest for the composition with the lowest fraction of chloroform ($CDCl_3$:CH-d_{12} 10%:90%), taking about 3 h at 343 K and 25 h on cooling to 293 K with less than 5% hydrolysis. When their NMR signals could not be integrated, the amounts of **Kn1** and **Kn3** were, respectively, calculated from those of their agonists **A3** and **A1**. There was almost no variation of composition when the solvent polarity was either too high (100% $CDCl_3$) or too low (10% $CDCl_3$ + 90% CH-d_{12}), indicating that no aggregation was occurring at high $CDCl_3$ fraction and that heating to 343 K was not sufficient to destroy the assemblies at the lowest $CDCl_3$ fraction. Only small shifts of the equilibrium were found below a 50%:50% solvent composition, which thus corresponds to the composition for which heating to 343 K is sufficient for melting of the supramolecular assemblies. In line with the titration results, above a composition of 30% $CDCl_3$ + 70% CH-d_{12}, the selectivity was highest and did not change anymore on increasing cyclohexane content (see Figure 1e,f for the ^{1}H NMR spectra). Taken together, the largest variation in distribution at equilibrium was from 24% **Kn1**, 24% **A3**, 26% **Kn3**, 26% **A1** to 6% **Kn1**, 6% **A3**, 44% **Kn3**, and 44% **A1**. Thus, both the constituent **Kn3** and consequently its agonistic constituent **A1** were subject to strong amplification driven by the sequential double self-organization first of **Kn3** into hydrogen-bonded hexameric rosettes, which set the stage for the subsequent assembly by stacking to generate the supramolecular polymer SP. The corresponding driving forces for **DCL-1** and **DCL-2** are calculated to be, respectively, 0.63 and 2.21 kcal/mol (see Table S1 for the free energies of all of the present DCLs, calculated following eq S1). The difference of about 1.6 kcal/mol between these two values indicates a markedly stronger stabilization of the SP aggregates, which may be attributed to the significantly longer spacer and the additional interactions introduced by the amide group in the side-chain of **Kn3**; it thus may well be considered as a third organizational driving force.

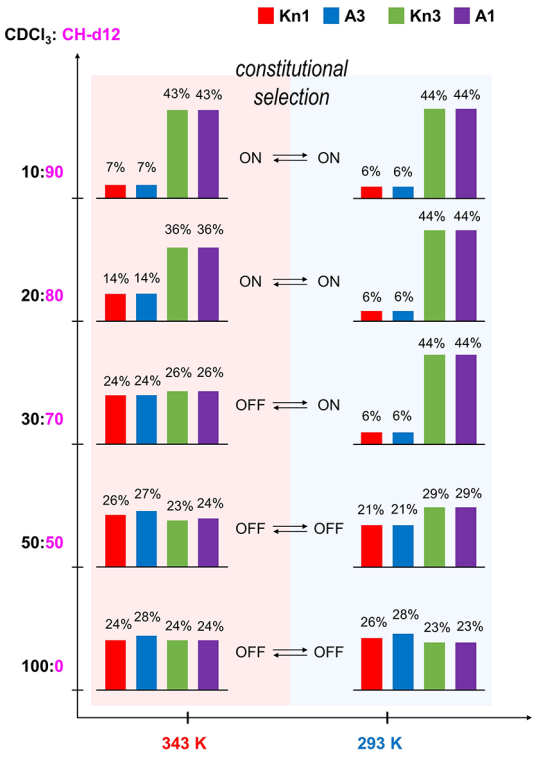

Figure 2. Representation of the variation in constitutional selectivity of **DCL-2** between 343 and 293 K as a function of solvent composition/polarity. The change from the "ON" state to "OFF" state represents the variation in constituent distribution driven by formation of the self-organized supramolecular aggregates. The time to reach equilibrium depends on the solvent composition and increases from bottom (30 min at 343 K and 90 min at 293 K) to top (3 h at 343 K and 25 h at 293 K). The error in % determination amounts to about 5%.

To better characterize the composition of the SP formed in **DCL-2**, the ^{1}H NMR data were analyzed in view of obtaining information about the amount of coassembly that may occur between **Kn1** and **Kn3** in the actual **DCL-2**. Considering the NMR spectrum shown in Figure 1f, as expected the signals of **Kn3** could not be observed because it was entirely contained in the supramolecular gel assembly. However, it was still possible to obtain the ratio **Kn1**:**Kn3** as 1:7.33 by comparing the integrals of the $=N-CH_2-$ peaks of their agonists **A3** and **A1**. Moreover, the $-OCH_2-$ peak of **Kn1** at 4.21 ppm remained observable, indicating that a certain amount of **Kn1** molecules were present as free molecules instead of participating in the coassembly with **Kn3**. From the amount of this free **Kn1** (0.7 with respect to **A3**), the ratio of free **Kn1** to total **Kn1** was found to be 0.7:1, giving a coassembly ratio **Kn1**:**Kn3** of 0.3:7.33. Thus, the SP formed in **DCL-2** consisted of a supramolecular coassembly composed of 96% **Kn1** and 4% **Kn3**. The ability of **Kn1** and **Kn3** themselves to coassemble was further investigated by mixing stoichiometric amounts of **Kn1** and **Kn3** in 30% $CDCl_3$ + 70% CH-d_{12}. As expected, the 400 MHz ^{1}H NMR spectrum (Figure S4a) did not show any **Kn3** signals, and only broad peaks of **Kn1** were observable, yielding an amount of free **Kn1** of 0.39 with respect to an internal standard (mesitylene). When the solvent composition of the sample was then tuned to 70% $CDCl_3$ + 30% CH-d_{12} by adding $CDCl_3$ (Figure S4b), all of the signals of **Kn1** and **Kn3** showed up as regular peaks in equal amounts of 0.59 with respect to the internal standard, yielding a composition of the coassembly of 25% **Kn1** + 75% **Kn3** (in Figure S4a).

https://doi.org/10.1021/jacs.1c04446
J. Am. Chem. Soc. XXXX, XXX, XXX−XXX

For comparison, the library **DCL-2′** (also in 30% $CDCl_3$ + 70% CH-d_{12}), which cannot lead to hydrogen bonding between the barbituric groups, was also examined. When a mixture of 2 mM **Kn1′** + **A3** was equilibrated at 70 °C, a statistical distribution of 25% was obtained for all four constituents (Figure 1g). After being cooled to 20 °C, the distribution underwent only a very small variation (22% **Kn1′**, 22% **A3**, 28% **Kn3′**, and 28% **A1**, Figure 1h). These results confirm the crucial role of the hydrogen-bonding-based self-assembly of the barbituric units into the hexameric rosettes.

The present **DCL-2** displays a larger distribution bias (6%, 6%, 44%, 44%) than the previously established two C═C/C═N DCLs: the DCL driven by addition of metal ions where a distribution of 8%, 9%, 42%, 40% was obtained as the chemical effector selected state,[16f] and the DCL driven by gelation of a specific constituent where a distribution of 10%, 9%, 40%, 40% was obtained as the physical stimulus selected state.[16d]

To investigate the reversibility of the dynamic system, **DCL-2** in 30% $CDCl_3$ + 70% CH-d_{12} was cyclically modulated between 343 and 293 K, and the evolution of the constituent distributions was monitored by ^{1}H NMR. The resulting changes in the ratio of (**A1**)/(**A3**) (obtained by ^{1}H NMR signal integration) as a function of time are shown in Figure 3

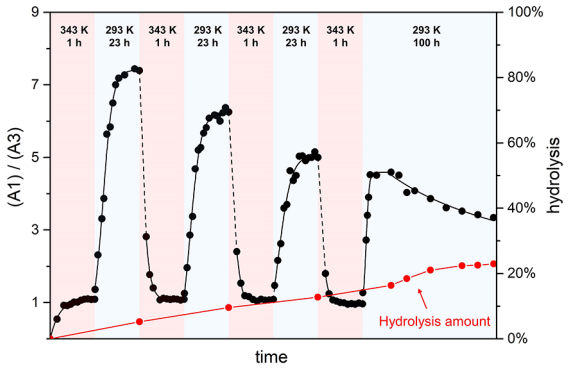

Figure 3. Reversible switching of the distribution of the constituents of **DCL-2** and adaptation as a function of temperature modulation in 30% $CDCl_3$ + 70% CH-d_{12}. (**A1**)/(**A3**) (left *Y* axis, black curve) and amount of hydrolysis products (%) versus time (right *Y* axis, red curve). Temperature and time scale of each pattern are annotated. (**A1**) and (**A3**) represent the amount of compound as obtained by integration of their CH═N and CH_2 signals in the ^{1}H NMR spectrum of the DCL. The error in % determination amounts to about 5%.

and indicate a good reversibility of the system. When the reaction solution was heated to 343 K, the equilibrium always displayed the selection "OFF" state ((**A1**)/(**A3**) ≈ 1) after 1 h, while after the solution was cooled to 293 K, the system underwent a slow (in about 20 h) variation in constituent distribution to the selection "ON" state (Scheme 2, center and right, Figure 2). The (**A1**)/(**A3**) selectivity in the "ON" states was gradually reduced from 7.4 (first cycle) to 5 (third cycle), and even to 3.4 (fourth cycle, after 100 h), a loss in reversibility that may be a consequence of the increasing hydrolysis of the constituents as indicated by the red curve in Figure 3 (see also Figure S5).

Electronic Spectroscopy Investigations of DCL-2. The dynamic behavior of **DCL-2** was also monitored by UV−vis spectrometry. The absorption spectra of the four constituents (1 mM) are shown in Figure 4a. **DCL-2** was obtained by mixing **Kn1** and **A3** (1 mM each) in 30% $CHCl_3$ + 70% CH.

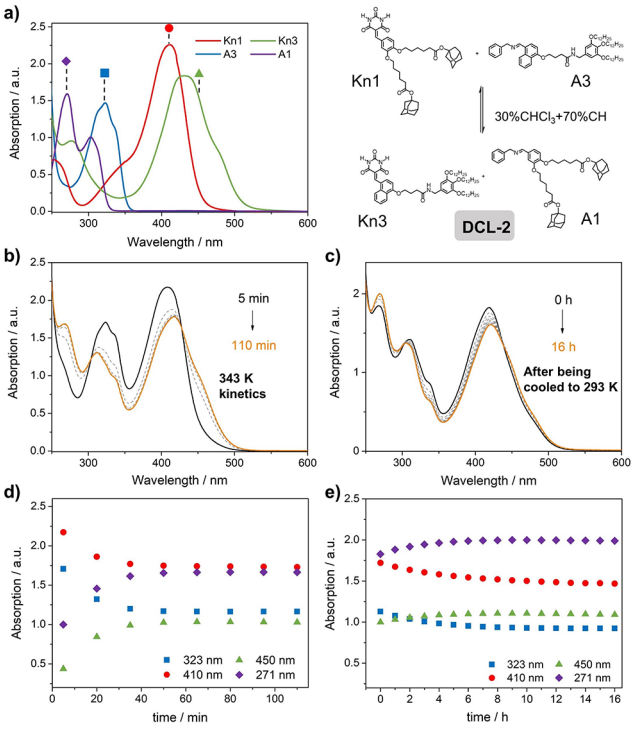

Figure 4. (a) UV−vis spectra of the four constituents of **DCL-2**, measured separately in 30% $CHCl_3$ + 70% CH (c = 1 mM, T = 293 K). UV−vis spectra of **DCL-2** starting from **Kn1**+**A1** (1 mM each): (b) spectra at 343 K, measured every 15 min; (c) spectra after cooling (0.5 K/min) to 293 K, measured every 1 h. Corresponding kinetic plots of absorptions at 271, 323, 410, and 450 nm of **DCL-2**: (d) at 343 K; (e) after cooling to 293 K. Before the UV−vis measurements, all of the samples were placed in 1 mm quartz cuvettes, used for the concentrated solutions, and sealed by parafilm.

The change in the absorption spectra of the reaction at 343 K is shown in Figure 4b. The absorptions at 323 and 410 nm, respectively, representing **A3** and **Kn1** decreased as the absorption at 271 and 450 nm, respectively, due to **A1** and **Kn3** increased (see Figure 4d for the changes observed at the four wavelengths versus time). From 65 to 110 min, no change was observed, which means the thermodynamic equilibrium was reached. After being cooled to 293 K (0.5 K/min), the DCL displayed continuous amplification of **Kn3** and **A1** in the first 12 h, as indicated by Figure 4c and e.

Structural Investigations of the Supramolecular Polymer SP by DLS, AFM, and Cryo-TEM. Dynamic light scattering (DLS) measurements of equilibrated **DCL-2** in 30% $CHCl_3$ + 70% CH at 293 K showed entities of an average hydrodynamic diameter (DH) of 31.52 nm with a polydispersity index (PDI) of 0.436 (see black curve in Figure 5a for the DLS of **DCL-2**). The single constituent solutions of **Kn1** and **Kn3** were also measured in the same conditions. The average D_H of **Kn3** (see red curve in Figure 5a) was 49.54 nm with a PDI of 0.240. The smaller object sizes and broader diameter region of **DCL-2**, as compared to **Kn3** alone, can be attributed to an adverse effect on the formation of supramolecular self-assemblies due to the participation/coassembly of the hindering bulky constituent **Kn1**. On the other hand, the correlogram (correlation coefficient versus time; see Figure S8

https://doi.org/10.1021/jacs.1c04446
J. Am. Chem. Soc. XXXX, XXX, XXX−XXX

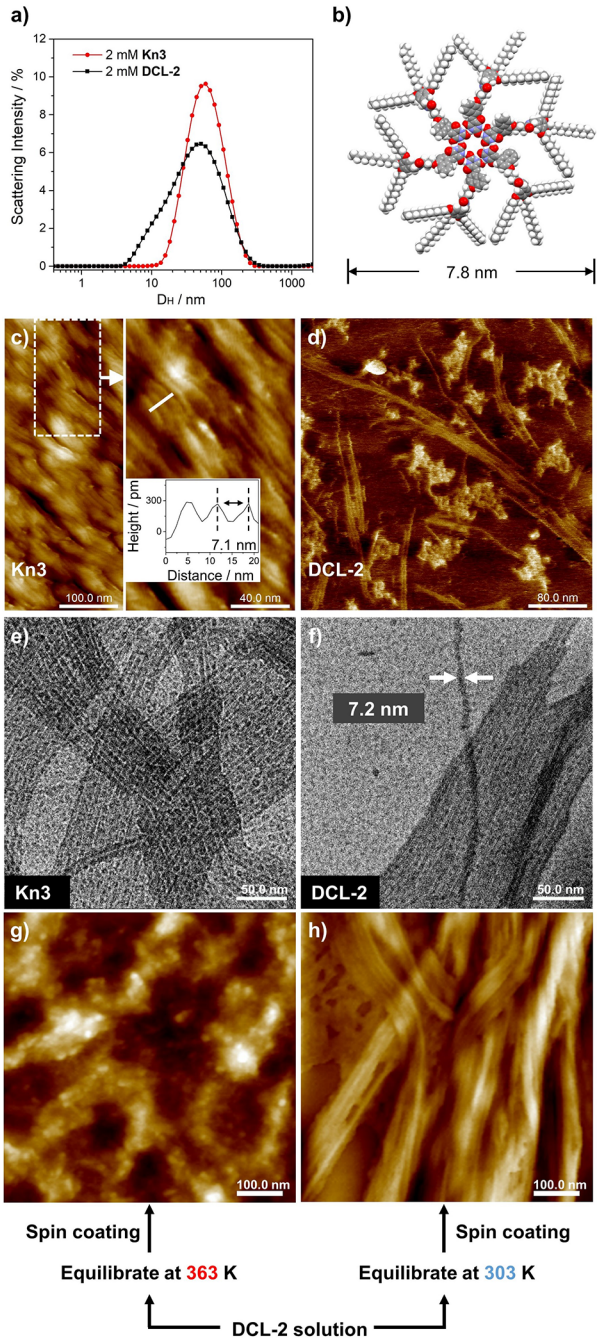

Figure 5. (a) DLS profiles of **DCL-2** and of **Kn3**, both in 30% $CHCl_3$ + 70% CH (c = 2 mM, T = 293 K). (b) Optimized computed structure for the rosette of **Kn3**, obtained using a semiempirical quantum mechanical GFN2-xTB method.[17] AFM images of (c) 1 mM **Kn3** in 30% $CHCl_3$ + 70% CH at 293 K (left) with (right) enlargement of the dashed box and cross-sectional analysis of the white solid line (inset); (d) 1 mM **DCL-2** in 30% $CHCl_3$ + 70% CH at 293 K; and 1 mM **DCL-2** in 30% $C_2H_2Cl_4$ + 70% MCH at (g) 363 K and (h) 303 K. Samples were spin-coated from equilibrated solutions onto HOPG. The AFM samples were dried under high vacuum for 1 week to ensure that no residual solvent remained on the plate. (e,f) Cryo-TEM micrographs (Titan-Krios) of (e) 0.1 mM **Kn3** at 293 K showing superimposed sheets of bundles of nanofibers of 6–7 nm diameter and (f) 0.1 mM **DCL-2** at 293 K showing a morphology similar to that in (e). Samples were drop-casted from 30% $CHCl_3$ + 70% CH equilibrated solutions onto graphene oxide grids.

for the correlograms of all of the present samples) for **Kn1** did not show a well-defined curve, pointing to the absence of supramolecular polymers. These DLS data not only supported the suggestion that **Kn1** itself does not form nanoscale supramolecular self-assemblies, but also indicated that the formation of supramolecular copolymers in **DCL-2** was driven by the self-assembly of **Kn3**.

The morphologies of the supramolecular self-assemblies were investigated by atomic force microscopy (AFM; Figure 5c,d) and cryogenic transmission electron microscopy (cryo-TEM; Figure 5g,h). The 1 mM 30% $CHCl_3$ + 70% CH solutions of **Kn3** and **DCL-2**, equilibrated at 293 K, were separately spin-coated onto highly oriented pyrolytic graphite (HOPG) for AFM imaging and drop-casted onto graphene oxide grids for cryo-TEM studies (see details in the Supporting Information).

The AFM images of **Kn3** (Figure 5c) showed bundled, parallel nanofibers with an average width of about 7 nm, in line with the diameter of 7.8 nm indicated by a computed geometry-optimized rosette structure of **Kn3** (Figure 5b; see the Supporting Information for details). In the same way, the cryo-TEM image of **Kn3** displayed overlapping nanosheets of crossed bundles of nanofibers (width 6–7 nm) in parallel arrangement (Figure 5e). Both AFM and cryo-TEM images of **Kn3** demonstrated the formation of supramolecular nanofibers, corresponding to our expectation of double supramolecular self-assembly as represented in Scheme 1b. For **DCL-2**, its AFM height image (Figure S9a) was blurry, probably caused by interference of nonassembled molecules of **A1** and **A2**. In comparison, its corresponding phase image (Figure 5d) clearly showed a mixture of disordered nanofibers with a wide range of lengths (5–340 nm, also in line with the DLS curve of **DCL-2** in Figure 5a), together with amorphous aggregates, probably due to the inclusion of molecules of the adamantane-bearing **Kn1** by some amount of copolymerization and resulting consequently in a perturbation in the stacking structure of the global supramolecular assemblies. The cryo-TEM image of **DCL-2** (Figure 5f) displayed bundled nanofibers (width 6–8 nm) similar to that of **Kn3** (Figure 5e), confirming that the constituent **Kn3** was selected as the dominating chemical species among the library. On the other hand, the cryo-TEM also recorded **DCL-2** (see Figure S9b) as less well-defined crossed nanofibers of larger complexity as one might expect in view of the possible incorporation of **Kn1** and the presence of the two other constituents **A1** and **A2** in the medium.

When the solution of **DCL-2** in 30% $C_2H_2Cl_4$ + 70% MCH was equilibrated at 363 K before being spin-coated onto HOPG, the corresponding AFM image (Figure 5g) shows only amorphous nanoparticles due to the full randomization of the constituents at high temperature. In comparison, when the same solution was equilibrated at 303 K before spin coating, the image obtained (Figure 5h) shows irregularly arranged nanofibers assembled and amorphous aggregates indicating both the major role of **Kn3** and the presence of the other three constituents.

Constituent Amplification and Component Selection at Low Reynolds Number. To establish the correlation between, on one hand, the level of medium organization reflected in frictional effects and bulk medium viscosity and, on the other hand, constituent amplification (component selection), ^{1}H NMR line widths (at half height $LW_{1/2}$) were determined as line broadening results from motional restriction

https://doi.org/10.1021/jacs.1c04446
J. Am. Chem. Soc. XXXX, XXX, XXX−XXX

in viscous media.[2] Thus, correlating signal line width with component amplification would establish selection at low Reynolds number, as an increase in viscosity corresponds to increasing supramolecular (passive) self-organization.

It is seen in Figure 1e that, when 30% $CDCl_3$ + 70% CH-d_{12} is used as the solvent of **DCL-2**, the supramolecular assemblies are not fully melted even at 343 K, as indicated by the broad **Kn3** peaks. Thus, to reach the gel to sol transition at a higher temperature, a mixed solvent of $C_2D_2Cl_4$ (deuterated 1,1,2,2-tetrachloroethane) and MCH-d_{14} (deuterated methylcyclohexane) was utilized. The double self-assembly behavior of the **Kn** compounds and the DCLs was then investigated under fine temperature control.

First, the solutions of 4 mM **Kn1** and **Kn3** in 30% $C_2D_2Cl_4$ + 70% MCH-d_{14} were, respectively, heated to 363 K in the NMR probe and then stepwise cooled to 303 K with stabilization at 11 intermediate temperatures (15 min each) for the recording of the 400 MHz ^{1}H NMR spectra (Figure 6a). As is seen (red spectra in Figure 6a), the H_a proton NMR signal of **Kn1** underwent a large shift from 7.9 to 9.1 ppm, indicating the gradual formation of the hexameric supramolecular rosettes by hydrogen bonding. There was almost no line-broadening during the cooling process, as indicated by the $LW_{1/2}$ of the H_b signal as a function of temperature shown in Figure 6c ($LW_{1/2}$ values obtained by the MNova software suite; see Figure S6 for details). Such a behavior is in line with our expectation that stacking of the rosettes of **Kn1** to form larger supramolecular assemblies would be sterically hindered. In comparison, the green spectra of **Kn3** (Figure 6a) show not only a large shift of the H_1 signal but also the broadening of all of the peaks. The $LW_{1/2}$ of H_2 (Figure 6c) underwent a sharp increase when the temperature was below 348 K, suggesting a critical temperature of supramolecular aggregation at about 348 K.

The solution of 4 mM **DCL-2** in 30% $C_2D_2Cl_4$ + 70% MCH-d_{14} was submitted to a similar procedure. At each temperature, the library was allowed to equilibrate until a stable distribution was obtained (see Figure 6b for the ^{1}H NMR spectra). The $LW_{1/2}$ values of the H_b and H_2 signals versus temperature are shown in Figure 6d. The curve of H_2 (**Kn3**) shows a sharp variation of the slope at about 348 K, in line with the green curve in Figure 6c. However, as compared to the H_b curve for **Kn1** alone where the line width barely changes, the curve of H_b (**Kn1**) in the **DCL-2** displays a different behavior with a growth in line width down from 348 K, indicating the participation of **Kn1** in stacking of the rosettes, by supramolecular copolymerization, which is also suggested by the less defined appearance of the assembled entities (Figure 5d). Furthermore, the variation of the equilibria of **DCL-2** under temperature cooling as illustrated by the black curve in Figure 6d for the ratio of (**A1**)/(**A3**) versus temperature (right *Y* axis) shows a synchronous trend with the line width variation of the H_b and H_2 signals as confirmed by the linear correlation between the (**A1**)/(**A3**) ratio and the H_b and H_2 signal line widths shown in Figure 6e.

On the other hand, bulk viscosity measurements (see the Supporting Information for details) showed that the logarithm of the specific viscosity of **DCL-2** (black curve in Figure 6f) also exhibits a change in slope at 343−348 K and a nonlinear growth under further cooling caused by both the increase in self-organization and the amplification of the concentration of **Kn3**. In comparison, the specific viscosity of **Kn1** solution (red curve in Figure 6f) was almost left unchanged upon cooling,

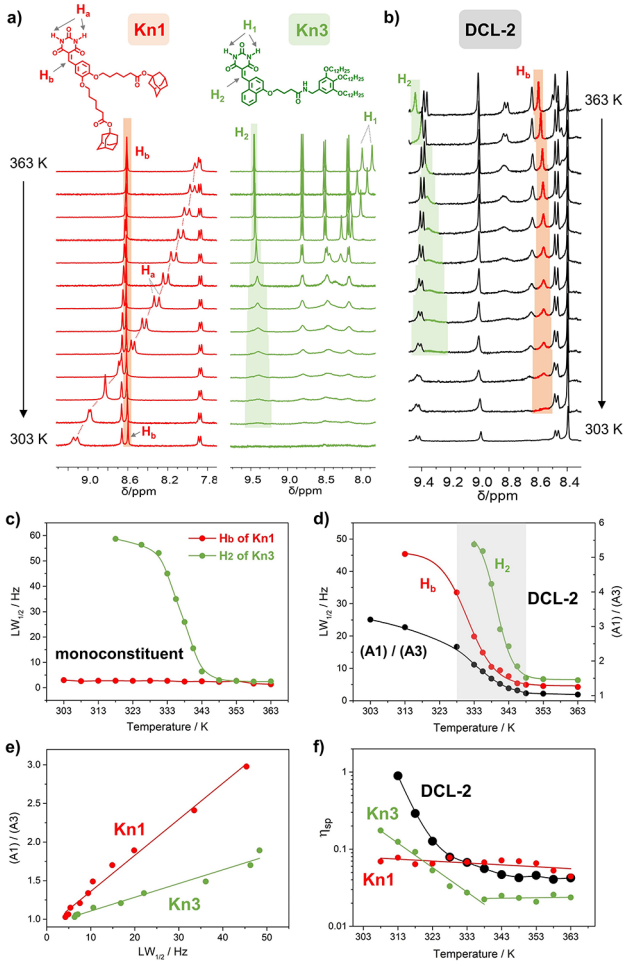

Figure 6. Partial 400 MHz ^{1}H NMR spectra of (a) single constituent solution of **Kn1** (left), **Kn3** (right) and (b) **DCL-2** under fine temperature control from 363 to 303 K (concentration, 4 mM; solvent, 30% $C_2D_2Cl_4$ + 70% MCH-d_{14}). (c) $LW_{1/2}$ (line width at half height in Hz) of H_b (**Kn1**) and H_2 (**Kn3**) in the single constituent Kn solution as a function of temperature data obtained from the spectra in (a). (d) $LW_{1/2}$ of H_b and H_2 in **DCL-2** as a function of temperature (left *Y* axis, data obtained from the spectra in (b)), (**A1**)/(**A3**) ratio versus temperature (black curve, right *Y* axis), and (e) (**A1**)/(**A3**) ratio as a function of $LW_{1/2}$. All of the $LW_{1/2}$ data were obtained using the MNova software suite, and the detailed procedure is described in Figure S6. (f) Logarithm of the specific viscosities of 4 mM **DCL-2** (black curve), 4 mM **Kn1** (red curve), and 4 mM **Kn3** (green curve) in 30% $C_2D_2Cl_4$ + 70% MCH-d_{14} as a function of temperature (see the Supporting Information for the detailed description of viscosity measurements). The green and red shaded areas in (a) and (b) represent the domains of line broadening. The full ^{1}H NMR spectra are shown in Figure S7.

while that of **Kn3** solution (green curve in Figure 6f) underwent a sharp linear growth after being cooled below 338 K as a result of self-organization.

Further information on the relation between macroscopic properties and microscopic behavior was obtained by rheological investigations of the mechanical properties of 4 mM **DCL-2** in 30% $C_2H_2Cl_4$ + 70% MCH (equilibrated at 298 K for 40 h) at 298 K. As shown in Figure 7a, it was found that the storage modulus (G') was larger than the loss modulus (G'') with small modulus values (~10 Pa) and that G' was independent of the angular frequency ω, indicating the formation of a soft organogel. Furthermore, the strain

https://doi.org/10.1021/jacs.1c04446
J. Am. Chem. Soc. XXXX, XXX, XXX−XXX

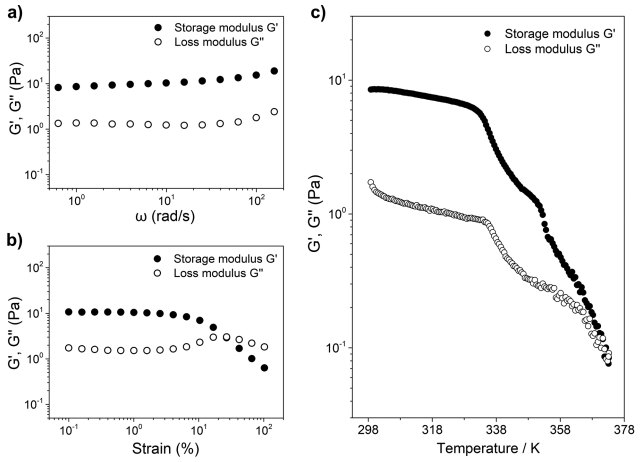

Figure 7. (a) Frequency dependence of G' (storage modulus) and G'' (loss molulus) of 4 mM **DCL-2** (equilibrated at 298 K for 40 h) with oscillation strain at 1%. (b) Dynamic strain sweep measurement with angular frequency at 6.28 rad/s of **DCL-2**. (c) Temperature dependence (293−374 K) of G' and G'' of **DCL-2**.

amplitude sweep in Figure 7b showed that there was a crossover of G' and G'' at 27% strain, demonstrating a disruption of the gel state. When the gel was gradually heated to 374 K (Figure 7c), the storage modulus underwent two sharp declines at 333 and 353 K, indicating a two-step decomposition of the supramolecular assemblies, which may be attributed, respectively, to the disruption of π stacking and hydrogen bonding. The crossover of G' and G'' at 373 K demonstrated a full phase transition of **DCL-2** from gel to solution.

CONCLUSION

We have here demonstrated the occurrence of self-organization-driven component selection and constituent amplification in the two DCLs, **DCL-1** and **DCL-2**, based on a dynamic covalent C═C/C═N organo-metathesis reaction. Constitutional adaptation in both DCLs is driven by a two-step sequential and conditional process involving first the formation of supramolecular rosettes, which conditions their subsequent stacking into a supramolecular polymeric entity SP, leading to the formation of a gel. It involves amplification of the thermodynamically favored constituent, that is, **Kn2** for **DCL-1** and **Kn3** for **DCL-2**, together with their constitutional agonist **A1**. The process is reversed with randomization of the constituents at elevated temperature on the gel to sol transition. Furthermore, the susceptibility of **DCL-2** to medium and to temperature results in diverse distribution patterns, showing a remarkable (fast) adaptivity to environmental information. Thus, DCLs based on C═C/C═N DCC may serve as a sensitive touchstone for the detection of perturbations by physical stimuli (temperature, pressure, fields) or chemical effectors (pH, ions, medium, etc.) through the shift in equilibrium distributions they cause.

Most significantly, the above studies involving NMR signal line widths, bulk medium features (viscosity, rheology), and dynamic equilibration in this complex system demonstrate the correlation between (passive) self-organization and constituent amplification under component selection. They thus unequivocally establish the phenomenon of self-organization-driven adaptation of a constitutional dynamic system. It may also operate in biological processes such as enzyme-catalyzed amino acid exchange and/or reshuffling in peptides and proteins. In general terms, self-organization-driven selection of those components that reinforce organization amounts to a self-amplification of organization toward soft matter systems of increasing complexity.[4] Overall, component selection, constituent amplification, and adaptation take place in a medium dominated by frictional effects and are thus enforced by low Reynolds number conditions.[1]

ASSOCIATED CONTENT

Supporting Information

The Supporting Information is available free of charge at https://pubs.acs.org/doi/10.1021/jacs.1c04446.

Details of instruments and measurements, synthetic procedures and characterization of the involved compounds, and supplementary data and figures (PDF)

AUTHOR INFORMATION

Corresponding Author

Jean-Marie Lehn − *Lehn Institute of Functional Materials, School of Chemistry, Sun Yat-Sen University, Guangzhou 510275, China; Laboratoire de Chimie Supramoléculaire, Institut de Science et d'Ingénierie Supramoléculaires (ISIS), Université de Strasbourg, Strasbourg 67000, France;* orcid.org/0000-0001-8981-4593; Email: lehn@unistra.fr

Author

Ruirui Gu − *Lehn Institute of Functional Materials, School of Chemistry, Sun Yat-Sen University, Guangzhou 510275, China; Laboratoire de Chimie Supramoléculaire, Institut de Science et d'Ingénierie Supramoléculaires (ISIS), Université de Strasbourg, Strasbourg 67000, France;* orcid.org/0000-0002-1831-7212

Complete contact information is available at: https://pubs.acs.org/10.1021/jacs.1c04446

Notes

The authors declare no competing financial interest.

ACKNOWLEDGMENTS

This study is dedicated to the memory of Edward M. Purcell in recognition of his inspiring paper.[1] We thank the ERC (Advanced Research Grant SUPRADAPT 290585), ANR DYNAFUN grant no. ANR-15-CE29-0009-01, and the University of Strasbourg Institute for Advanced Study (USIAS) for financial support. We thank Dr. Jean-Louis Schmitt and Dr. Cyril Antheaume for discussions of the NMR and mass spectral data and Dr. Artem Osypenko for extensive discussions. This work was also supported by the Integrated Structural Biology Platform at the Centre for Integrative Biology/IGBMC, by the French Infrastructure for Integrated Structural Biology (FRISBI) ANR-10-INSB-05-01, and by Instruct-ERIC, and we thank Dr. Brice Beinsteiner and Dr. Bruno Klaholtz for the cryo-TEM analysis. We are very grateful to Dr. Li Gong (SYSU) and Ye Wang (ISIS) for the AFM imaging and Dr. Wende Hu (Shanghai) for the computational results. R.G. gratefully acknowledges a postdoctoral fellowship from Sun-Yat Sen University and financial support from the China Postdoctoral Science Foundation.

https://doi.org/10.1021/jacs.1c04446
J. Am. Chem. Soc. XXXX, XXX, XXX−XXX

REFERENCES

(1) Purcell, E. M. Life at Low Reynolds Number. *Am. J. Phys.* **1977**, *45*, 3−11.

(2) Bloembergen, N.; Purcell, E. M.; Pound, R. V. Relaxation Effects in Nuclear Magnetic Resonance Absorption. *Phys. Rev.* **1948**, *73*, 679−712.

(3) Lehn, J.-M. Perspectives in Chemistry−Steps towards Complex Matter. *Angew. Chem., Int. Ed.* **2013**, *52*, 2836−2850.

(4) Lehn, J.-M. Toward Complex Matter: Supramolecular Chemistry and Self-Organization. *Proc. Natl. Acad. Sci. U. S. A.* **2002**, *99*, 4763−4768.

(5) De Gennes, P.-G. Soft Matter (Nobel Lecture). *Angew. Chem., Int. Ed. Engl.* **1992**, *31*, 842−845.

(6) (a) Lehn, J.-M. From Supramolecular Chemistry towards Constitutional Dynamic Chemistry and Adaptive Chemistry. *Chem. Soc. Rev.* **2007**, *36*, 151−160. (b) Corbett, P. T.; Leclaire, J.; Vial, L.; West, K. R.; Wietor, J.-L.; Sanders, J. K. M.; Otto, S. Dynamic Combinatorial Chemistry. *Chem. Rev.* **2006**, *106*, 3652−3711. (c) Ladame, S. Dynamic Combinatorial Chemistry: on the Road to Fulfilling the Promise. *Org. Biomol. Chem.* **2008**, *6*, 219−226. (d) Lehn, J.-M. Perspectives in Chemistry−Aspects of Adaptive Chemistry and Materials. *Angew. Chem., Int. Ed.* **2015**, *54*, 3276−3289. (e) Belowich, M. E.; Stoddart, J. F. Dynamic Imine Chemistry. *Chem. Soc. Rev.* **2012**, *41*, 2003−2024.

(7) (a) Black, S. P.; Sanders, J. K. M.; Stefankiewicz, A. R. Disulfide Exchange: Exposing Supramolecular Reactivity through Dynamic Covalent Chemistry. *Chem. Soc. Rev.* **2014**, *43*, 1861−1872. (b) Liu, B.; Pappas, C. G.; Zangrando, E.; Demitri, N.; Chmielewski, P. J.; Otto, S. Complex Molecules That Fold Like Proteins Can Emerge Spontaneously. *J. Am. Chem. Soc.* **2019**, *141*, 1685−1689.

(8) Ruff, Y.; Garavini, V.; Giuseppone, N. Reversible Native Chemical Ligation: A Facile Access to Dynamic Covalent Peptides. *J. Am. Chem. Soc.* **2014**, *136*, 6333−6339.

(9) Lu, Y.-X.; Guan, Z. Olefin Metathesis for Effective Polymer Healing via Dynamic Exchange of Strong Carbon−Carbon Double Bonds. *J. Am. Chem. Soc.* **2012**, *134*, 14226−14231.

(10) (a) Chen, X.; Dam, M. A.; Ono, K.; Mal, A.; Shen, H.; Nutt, S. R.; Sheran, K.; Wudl, F. A Thermally Re-mendable Cross-Linked Polymeric Material. *Science* **2002**, *295*, 1698−1702. (b) Boul, P.; Reutenauer, P.; Lehn, J.-M. Reversible Diels−Alder Reactions for the Generation of Dynamic Combinatorial Libraries. *Org. Lett.* **2005**, *7*, 15−18. (c) Sun, H.; Kabby, C. P.; Dai, Y.; Hill, M. R.; Ghiviriga, I.; Bapat, A. P.; Sumerlin, B. S. Macromolecular Metamorphosis via Stimulus-Induced Transformations of Polymer Architecture. *Nat. Chem.* **2017**, *9*, 817−823.

(11) (a) Kulchat, S.; Meguellati, K.; Lehn, J.-M. Organocatalyzed and Uncatalyzed C = C/C = C and C = C/C = N Exchange Processes between Knoevenagel and Imine Compounds in Dynamic Covalent Chemistry. *Helv. Chim. Acta* **2014**, *97*, 1219−1236. (b) Gu, R.; Flidrova, K.; Lehn, J.-M. Dynamic Covalent Metathesis in the C = C/C = N Exchange between Knoevenagel Compounds and Imines. *J. Am. Chem. Soc.* **2018**, *140*, 5560−5568.

(12) (a) Aida, T.; Meijer, E. W.; Stupp, S. I. Functional Supramolecular Polymers. *Science* **2012**, *335*, 813−817. (b) Mattia, E.; Otto, S. Supramolecular Systems Chemistry. *Nat. Nanotechnol.* **2015**, *10*, 111−119. (c) Moulin, E.; Armao, J. J.; Giuseppone, N. Triarylamine-Based Supramolecular Polymers: Structures, Dynamics, and Functions. *Acc. Chem. Res.* **2019**, *52*, 975−983. (d) Sorrenti, A.; Leira-Iglesias, J.; Markvoort, A. J.; De Greef, T. F. A.; Hermans, T. M. Non-Equilibrium Supramolecular Polymerization. *Chem. Soc. Rev.* **2017**, *46*, 5476−5490. (e) Li, C.; Iscen, A.; Sai, H.; Sato, K.; Sather, N. A.; Chin, S. M.; Álvarez, Z.; Palmer, L. C.; Schatz, G. C.; Stupp, S. I. Supramolecular-Covalent Hybrid Polymers for Light-Activated Mechanical Actuation. *Nat. Mater.* **2020**, *19*, 900−909. (f) Rao, S. J.; Zhang, Q.; Mei, J.; Ye, X. H.; Gao, C.; Wang, Q. C.; Qu, D. H.; Tian, H. One-Pot Synthesis of Hetero[6]rotaxane Bearing Three Different Kinds of Macrocycle through A Self-Sorting Process. *Chem. Sci.* **2017**, *8*, 6777−6783. (g) Rizzuto, F. J.; Nitschke, J. R. Narcissistic, Integrative, and Kinetic Self-Sorting within a System of Coordination Cages. *J. Am. Chem. Soc.* **2020**, *142*, 7749−7753. (h) Wang, G. T.; Lin, J. B.; Jiang, X. K.; Li, Z. T. Cholesterol-Appended Aromatic Imine Organogelators: A Case Study of Gelation-Driven Component Selection. *Langmuir* **2009**, *25*, 8414−8418. (i) Zhang, Q.; Deng, Y. X.; Luo, H. X.; Shi, C. Y.; Geise, G. M.; Feringa, B. L.; Tian, H.; Qu, D. H. Assembling a Natural Small Molecule into a Supramolecular Network with High Structural Order and Dynamic Functions. *J. Am. Chem. Soc.* **2019**, *141*, 12804−12814.

(13) (a) Fouquey, C.; Lehn, J.-M.; Levelut, A.-M. Molecular Recognition Directed Self-Assembly of Supramolecular Liquid Crystalline Polymers from Complementary Chiral Components. *Adv. Mater.* **1990**, *2*, 254−257. (b) Lehn, J.-M.; Mascal, M.; Decian, A.; Fischer, J. Molecular Recognition Directed Self-Assembly of Ordered Supramolecular Strands by Cocrystallization of Complementary Molecular Components. *J. Chem. Soc., Chem. Commun.* **1990**, 479−481. (c) Ghadiri, M. R.; Granja, J. R.; Milligan, R. A.; McRee, D. E.; Khazanovich, N. Self-Assembling Organic Nanotubes Based on A Cyclic Peptide Architecture. *Nature* **1993**, *366*, 324−327. (d) Marsh, A.; Silvestri, M.; Lehn, J.-M. Self-Complementary Hydrogen Bonding Heterocycles Designed for the Enforced Self-Assembly into Supramolecular Macrocycles. *Chem. Commun.* **1996**, *13*, 1527−1528. (e) Fenniri, H.; Mathivanan, P.; Vidale, K. L.; Sherman, D. M.; Hallenga, K.; Wood, K. V.; Stowell, J. G. Helical Rosette Nanotubes: Design, Self-Assembly, and Characterization. *J. Am. Chem. Soc.* **2001**, *123*, 3854−3855. (f) Bielejewska, A. G.; Marjo, C. E.; Prins, L. J.; Timmerman, P.; De Jong, F.; Reinhoudt, D. N. Thermodynamic Stabilities of Linear and Crinkled Tapes and Cyclic Rosettes in Melamine-Cyanurate Assemblies: A Model Description. *J. Am. Chem. Soc.* **2001**, *123*, 7518−7533. (g) Prins, L. J.; De Jong, F.; Timmerman, P.; Reinhoudt, D. N. An Enantiomerically Pure Hydrogen-Bonded Assembly. *Nature* **2000**, *408*, 181−184. (h) Chang, S. K.; Hamilton, A. D. Molecular Recognition of Biologically Interesting Substrates: Synthesis of An Artificial Receptor for Barbiturates Employing Six Hydrogen Bonds. *J. Am. Chem. Soc.* **1988**, *110*, 1318−1319. (i) Chang, S. K.; Van Engen, D.; Fan, E.; Hamilton, A. D. Hydrogen Bonding and Molecular Recognition: Synthetic, Complexation, and Structural Studies on Barbiturate Binding to An Artificial Receptor. *J. Am. Chem. Soc.* **1991**, *113*, 7640−7645. (j) Berl, V.; Schmutz, M.; Krische, M. J.; Khoury, R. G.; Lehn, J.-M. Supramolecular Polymers Generated from Heterocomplementary Monomers Linked through Multiple Hydrogen-Bonding Arrays− Formation, Characterization, and Properties. *Chem. - Eur. J.* **2002**, *8*, 1227−1244.

(14) (a) Aida, T.; Meijer, E. W. Supramolecular Polymers − we've Come Full Circle. *Isr. J. Chem.* **2020**, *60*, 33−47. (b) Korevaar, P. A.; George, S. J.; Markvoort, A. J.; Smulders, M. M. J.; Hilbers, P. A. J.; Schenning, A. P. H. J.; De Greef, T. F. A.; Meijer, E. W. Pathway Complexity in Supramolecular Polymerization. *Nature* **2012**, *481*, 492−496. (c) Kang, J.; Miyajima, D.; Mori, T.; Inoue, Y.; Itoh, Y.; Aida, T. A Rational Strategy for the Realization of Chain-Growth Supramolecular Polymerization. *Science* **2015**, *347*, 646−651. (d) Armao, J. J.; Maaloum, M.; Ellis, T.; Fuks, G.; Rawiso, M.; Moulin, E.; Giuseppone, N. Healable Supramolecular Polymers as Organic Metals. *J. Am. Chem. Soc.* **2014**, *136*, 11382−11388. (e) Adelizzi, B.; Aloi, A.; Markvoort, A. J.; Ten Eikelder, H. M. M.; Voets, I. K.; Palmans, A. R. A.; Meijer, E. W. Supramolecular Block Copolymers under Thermodynamic Control. *J. Am. Chem. Soc.* **2018**, *140*, 7168−7175. (f) Korevaar, P. A.; Schaefer, C.; De Greef, T. F. A.; Meijer, E. W. Controlling Chemical Self-Assembly by Solvent-Dependent Dynamics. *J. Am. Chem. Soc.* **2012**, *134*, 13482−13491. (g) Đorđević, L.; Marangoni, T.; Miletić, T.; Rubio-Magnieto, J.; Mohanraj, J.; Amenitsch, H.; Pasini, D.; Liaros, N.; Couris, S.; Armaroli, N.; Surin, M.; Bonifazi, D. Solvent Molding of Organic Morphologies Made of Supramolecular Chiral Polymers. *J. Am. Chem. Soc.* **2015**, *137*, 8150−8160.

(15) (a) Yagai, S.; Goto, Y.; Lin, X.; Karatsu, T.; Kitamura, A.; Kuzuhara, D.; Yamada, H.; Kikkawa, Y.; Saeki, A.; Seki, S. Self-Organization of Hydrogen-Bonding Naphthalene Chromophores into J-type Nanorings and H-type Nanorods: Impact of Regioisomerism. *Angew. Chem., Int. Ed.* **2012**, *51*, 6643−6647. (b) Yagai, S.; Kitamoto,

https://doi.org/10.1021/jacs.1c04446
J. Am. Chem. Soc. XXXX, XXX, XXX−XXX

Y.; Datta, S.; Adhikari, B. Supramolecular Polymers Capable of Controlling Their Topology. *Acc. Chem. Res.* **2019**, *52*, 1325−1335. (c) Datta, S.; Kato, Y.; Higashiharaguchi, S.; Aratsu, K.; Isobe, A.; Saito, T.; Prabhu, D. D.; Kitamoto, Y.; Hollamby, M. J.; Smith, A. J.; Dagleish, R.; Mahmoudi, N.; Pesce, L.; Perego, C.; Pavan, G. M.; Yagai, S. Self-Assembled Poly-Catenanes from Supramolecular Toroidal Building Blocks. *Nature* **2020**, *583*, 400−405. (d) Aratsu, K.; Takeya, R.; Pauw, B. R.; Hollamby, M. J.; Kitamoto, Y.; Shimizu, N.; Takagi, H.; Haruki, R.; Adachi, S.; Yagai, S. Supramolecular Copolymerization Driven by Integrative Self-sorting of Hydrogen-Bonded Rosettes. *Nat. Commun.* **2020**, *11*, 1−12.

(16) (a) Sreenivasachary, N.; Lehn, J.-M. Gelation-Driven Component Selection in the Generation of Constitutional Dynamic Hydrogels Based on Guanine-Quartet Formation. *Proc. Natl. Acad. Sci. U. S. A.* **2005**, *102*, 5938−5943. (b) Nguyen, R.; Allouche, L.; Buhler, E.; Giuseppone, N. Dynamic Combinatorial Evolution within Self-Replicating Supramolecular Assemblies. *Angew. Chem., Int. Ed.* **2009**, *48*, 1093−1096. (c) Minkenberg, C. B.; Li, F.; van Rijn, P.; Florusse, L.; Boekhoven, J.; Stuart, M. C. A.; Koper, G. J. M.; Eelkema, R.; van Esch, J. H. Responsive Vesicles from Dynamic Covalent Surfactants. *Angew. Chem., Int. Ed.* **2011**, *50*, 3421−3424. (d) Liang, C.; Kulchat, S.; Jiang, S.; Lehn, J.-M. Gelation-Driven Selection in Dynamic Covalent C = C/C = N Exchange. *Chem. Sci.* **2017**, *8*, 6822−6828. (e) Seoane, A.; Brea, R. J.; Fuertes, A.; Podolsky, K. A.; Devaraj, N. K. Biomimetic Generation and Remodeling of Phospholipid Membranes by Dynamic Imine Chemistry. *J. Am. Chem. Soc.* **2018**, *140*, 8388−8391. (f) Gu, R.; Lehn, J.-M. Metal Ion-Driven Constitutional Adaptation in Dynamic Covalent C = C/C = N Organo-Metathesis. *Chem. - Asian J.* **2021**, *16*, 44−48.

(17) Bannwarth, C.; Ehlert, S.; Grimme, S. GFN2-xTB−An Accurate and Broadly Parametrized Self-Consistent Tight-Binding Quantum Chemical Method with Multipole Electrostatics and Density-Dependent Dispersion Contributions. *J. Chem. Theory Comput.* **2019**, *15*, 1652−1671.

https://doi.org/10.1021/jacs.1c04446
J. Am. Chem. Soc. XXXX, XXX, XXX−XXX